The oxidative capacity of the troposphere: Coupling of field measurements of OH and a global chemistry transport model

William J. Bloss,*[a] Mathew J. Evans,[b] James D. Lee,[c] Roberto Sommariva,[a] Dwayne E. Heard[a] and Michael J. Pilling[a]

[a] *School of Chemistry, University of Leeds, Leeds, UK, LS2 9JT. E-mail: w.j.bloss@chemistry.leeds.ac.uk*
[b] *School of Earth and Environment, University of Leeds, Leeds, UK, LS2 9JT*
[c] *Department of Chemistry, University of York, Heslington, York, UK, YO10 5DD*

Received 20th December 2004, Accepted 7th February 2005
First published as an Advance Article on the web 29th June 2005

A combination of *in situ*, ground-based observations of marine boundary layer OH concentrations performed by laser-induced fluorescence at Mace Head, Ireland and Cape Grim, Tasmania, and a global chemistry-transport model (GEOS-CHEM) are used to obtain an estimate of the mean concentration of OH in the global troposphere. The model OH field is constrained to the geographically sparse, observed OH concentration averaged over the duration of the measurement campaigns to remove diurnal and synoptic variability. The mean northern and southern hemispheric OH concentrations obtained are 0.91×10^6 cm^{-3} and 1.03×10^6 cm^{-3} respectively, consistent with values determined from methyl chloroform observations. The observational OH dataset is heavily biased towards mid-latitude summer and autumn observations in the northern hemisphere, while the global oxidising capacity is dominated by the tropics which is observed extremely sparsely; the implications of these geographical distributions are discussed.

1. Introduction

The physical and chemical properties of the atmosphere are influenced by the presence of atmospheric species present at trace concentrations, such as greenhouse gases, influencing radiative transfer and hence climate, hydrocarbons and oxides of nitrogen affecting urban air quality, and chlorofluorocarbons which impact upon the ozone layer. The oxidative capacity of the atmosphere determines the rate of removal, and hence controls the abundance, of most trace gas species. For species such as CH_4, CO and non-methane hydrocarbons (NMHC), oxidation is initiated overwhelmingly by reaction with the hydroxyl radical, OH, in the troposphere.[1] Understanding of the concentrations and distribution of tropospheric OH is therefore of fundamental importance to both atmospheric chemistry and climate science.

The reaction of trace gas species with OH initiates a chain of degradation steps which ultimately result in their removal from the atmosphere or their oxidation to carbon dioxide and water. The OH radical is highly reactive, with a chemical lifetime of the order of 0.1–1 s; consequently OH concentrations are extremely low, of the order of $(0.5–5) \times 10^6$ cm^{-3} in the boundary layer. Reliable direct measurement of OH is challenging; however a number of successful *in situ* observations have been made using techniques including laser-induced fluorescence, differential optical absorption

spectroscopy and chemical ionisation-mass spectrometry (*e.g.* Heard and Pilling[2] and references therein) and there exists a body of observational data at a limited number of point measurement sites.

As a consequence of the short chemical lifetime of OH, local chemistry rather than transport determines OH concentrations. Thus, observationally constrained box models which ignore transport are well suited to analysis of OH measurements. These models are typically constrained to measured concentrations of long-lived species such as hydrocarbons, oxides of nitrogen and ozone (O_3), together with physical parameters, and by various approaches to the forward integration calculate a concentration of OH to compare with the observations. Such studies can provide understanding of the processes controlling OH locally but provide little or no information about the global distribution of OH.[2]

An alternative approach to determine the global abundance and distribution of OH is to employ observations of trace gases such as methyl chloroform (CH_3CCl_3) which are predominantly destroyed through reaction with OH. Through inverse modelling techniques using a chemistry transport model, a mean atmospheric OH concentration can be derived.[3–7] Such global mean concentrations are suitable for comparison with global atmospheric chemistry transport models and provide an assessment in the broadest sense of the global oxidation within a model. They do however suffer from some difficulties: the combination of a relatively sparse observational network, long lifetimes (relative to the appropriate transport timescales) and uncertainties in the emissions data, places some constraints upon the global validity of the OH values obtained.[8]

Given the importance the oxidizing capacity of the atmosphere to climate, checking the consistency of both 'bottom-up' (from *in situ* observations of OH) and 'top-down' (from tracer inversion) approaches is important. In this paper we provide an initial attempt to best use a sparse set of direct observations of OH (both the northern and southern hemispheres) together with a global model of atmospheric chemistry and transport to provide a novel constraint on the global atmospheric burden of OH. We then evaluate the uncertainties in the observational constraint and suggest a variety of future observational strategies that may help to reduce the uncertainty in the global distribution of OH. We conclude that focusing observational effort on the tropical lower atmosphere would provide a significant enhancement of our knowledge of the current and future global oxidizing capacity.

2. Observations

In this work we use OH data acquired *in situ*, at ground level, by the University of Leeds HO_x measurement system, during three field campaigns at coastal sites: EASE97, SOAPEX-2 and NAMBLEX. The EASE97 (East Atlantic Spring Experiment 1997) and NAMBLEX (North Atlantic Marine Boundary Layer Experiment) campaigns were both conducted at Mace Head Atmospheric Research Station, Co. Galway, Ireland (53° 19′ 34″ N, 9° 54′ 14″ W), from 26th April–25th May 1997 and 20th July–3rd September 2002, respectively. The SOAPEX-2 (Southern Ocean Atmospheric Photochemistry Experiment 2) campaign was conducted at Cape Grim Baseline Atmospheric Pollution Station, Tasmania (40° 46′ 56″ S, 144° 41′ 18″ E) from 18th January to 18th February 1999. The Mace Head Atmospheric Research Station, a part of the Advanced Global Atmospheric Gases Experiment (AGAGE) and a WMO Global Atmospheric Watch station, is located on the remote west coast of Ireland, and experiences prevailing marine air from the Atlantic Ocean between 180° and 300°. The OH measurements were made at the "shoreline site", located 50 m behind the high water mark, at an inlet height of 10 m above mean sea level. The Cape Grim Baseline Atmospheric Pollution Station, also a GAW station, is located on the north-western coast of Tasmania, on a cliff top 100 m above mean sea level. The OH measurements were made approximately 80 m horizontally from the high water mark. The Mace Head and Cape Grim sites are described in more detail in refs. 9 and 10, respectively.

The dataset used is not a comprehensive set of the available OH observations; for simplicity we have used only single-location (hence ground-based) datasets, from marine locations where chemical complexity and small-scale inhomogeneity are expected to be minimised. Future developments may allow inclusion of aircraft- or ship-borne observations. The spatial distribution of the available HO_x data is addressed further in section 5.

The University of Leeds OH measurement system, which uses the LIF (laser induced fluorescence) technique employing the FAGE (fluorescence assay by gas expansion) methodology,[11] has been described in detail previously.[12–14] LIF is not an absolute technique, thus the instrument sensitivity must be determined. The response of the Leeds LIF system was determined by the water photolysis–O_3 actinometry method,[15] in which the 184.9 nm photolysis of a flow of humidified air leads to the formation of OH and HO_2 in equal concentrations, which can be determined relative to the concomitant formation of O_3 from O_2 photolysis.

The humidity of the air entering the calibration system is known, and used in conjunction with measurement of the O_3 concentration and relevant cross sections and quantum yields to calculate the concentration of OH or HO_2 radicals formed. The overall uncertainty in an individual measurement of OH has been calculated to be 26% (one standard deviation),[16] however the principal source of this uncertainty is the measurement of the O_3 concentration, in particular the determination of the instrument zero. In the present work, where the mean OH concentration averaged over a four to six week campaign are compared with their modelled equivalents, this source of uncertainty will impact the *precision* of the OH measurements, rather than their systematic accuracy, as multiple calibrations are performed during every day of the measurement campaigns. We therefore estimate the systematic uncertainty in the ensemble OH data to be 13% (one standard deviation).

3. Model

The GEOS-CHEM model of atmospheric composition is a global atmospheric chemistry/aerosol transport model. It has been extensively validated and used to study a variety of atmospheric phenomena (*e.g.* refs. 17–20). For this work, we use Version 6-5-02 (see http://io.harvard.edu/chemistry/trop/geos/index.html) and run the model for two years (2000–2002) at a coarse resolution of $4^\circ \times 5^\circ$. The first year is taken as spin-up and is not considered further. Output of concentrations of key species is made every hour at Mace Head, Ireland and Cape Grim, Tasmania.

Fig. 1 compares the global annual mean tropospheric mass weighted OH concentration determined by GEOS-CHEM with that from various indirect observational determinations. The observational data[4–7] are typically determined from measurements of long-lived tracer species such as methyl chloroform (whose emissions are thought to be well constrained), or computed from measured global distributions of O_3, NO_x, hydrocarbons *etc*.[21] The temporally and globally integrated OH calculated by the GEOS-CHEM model is consistent with the observational determinations; however, given the variability between, and the quoted uncertainties of the observational studies, this does not provide a wholly conclusive test of the model. The mean OH concentration obtained from the observationally derived seasonal averages shown in Fig. 1 is $(1.04 \pm 0.13) \times 10^6$ cm^{-3}. The equivalent value from the GEOS-CHEM model is $(1.07 \pm 0.03) \times 10^6$ cm^{-3}.

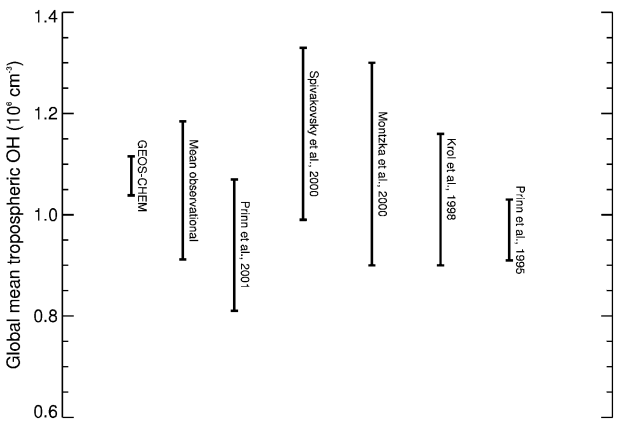

Fig. 1 Global mean annual tropospheric OH, calculated by the GEOS-CHEM model (for which error bars show the standard deviation of monthly mean values from the annual mean) and values determined by various observational studies.

The model quoted uncertainty reflects variability in the calculated monthly mean OH concentration over the year rather than the uncertainty in the model, which is likely to be much higher. Some sense of the model uncertainty can be gauged from the variability of this value over different model versions (see http://io.harvard.edu/chemistry/trop/geos/geos_versions.html) which ranges from 0.99×10^6 to 1.17×10^6 cm^{-3}.

The Prinn *et al.*[6] study gives hemispheric mean OH values of $(0.90 \pm 0.20) \times 10^6$ cm^{-3} and $(0.99 \pm 0.20) \times 10^6$ cm^{-3} for the northern and southern hemisphere, respectively. GEOS-CHEM simulates values of 1.12×10^6 cm^{-3} and 1.02×10^6 cm^{-3} for the northern and southern hemisphere, respectively. Thus, the indirect observations suggest higher OH concentrations within the southern hemisphere than the northern, whereas the model simulates the opposite.

4. Model comparison with OH measurement data

Fig. 2 shows a comparison between observed concentrations of OH and those calculated using the GEOS-CHEM model over the period of the NAMBLEX campaign (Mace Head, Ireland; July–September 2002). Unsurprisingly, the model resolves the day/night variability seen in the observations and is to some extent capable of resolving those days with high concentrations from those with low. Fig. 3 shows the direct comparison between the hourly mean observed OH concentrations and those calculated by the model (there are 802 data points). The model overestimates the observations (measured mean is 1.8×10^6 cm^{-3}, modelled mean is 2.3×10^6 cm^{-3}) with a mean model to measured ratio of 1.56 ± 1.62. The statistical distribution of the ratio is not normal and so more appropriate metrics such as the median (1.13) or the geometric mean ($1.13^{+1.44}_{-0.64}$), provide a more robust assessment of the model skill. The model simulates 30% of the variability of OH (as defined by the R^2). The model therefore has some skill in simulating the OH concentration. Given the uncertainty in the observations (13% as discussed above) the model does appear to systematically overestimate the measured OH concentrations.

The model simulation of the observed data is in some respects surprising, as a growing body of evidence indicates that the Mace Head measurement site may be atypical of the open ocean marine boundary layer, owing to emissions of halogen, particularly iodine, species from macro-algae in the littoral zone;[22,23] the GEOS-CHEM model does not include any halogen chemistry. Broadly, the presence of a large photolabile iodine source is expected to affect the HO_x photochemistry principally by reacting with HO_2 to form HOI, which can then be removed due to heterogeneous processes or photolysed to release OH. These processes may have a significant impact upon HO_2, however their effect upon OH is limited, at the levels observed, as OH formation is overwhelmingly

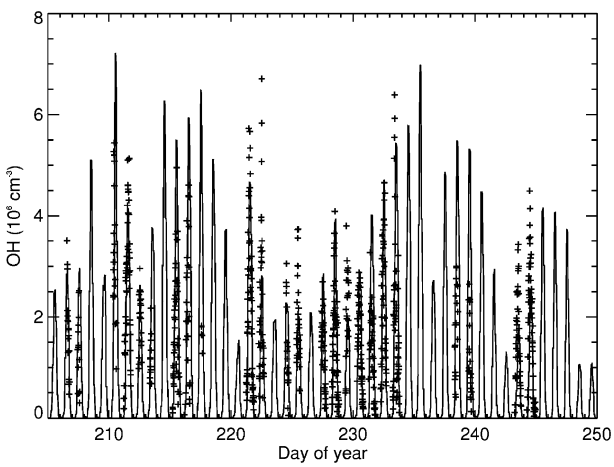

Fig. 2 Measured OH concentrations at Mace Head, Ireland during the 2002 NAMBLEX campaign (crosses) and OH concentrations calculated by the GEOS-CHEM model (continuous line). Measured data shown are hourly averages of (typically) 10–12 individual measurements; all measured data is shown: gaps indicate instrumental difficulties.

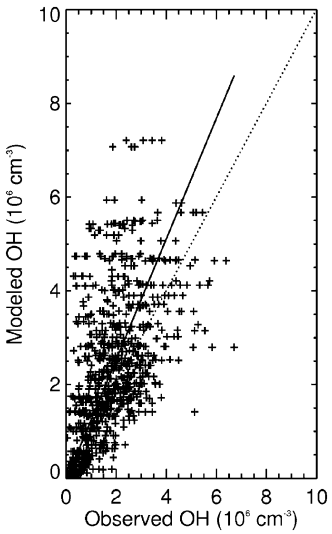

Fig. 3 Comparison of observed and modelled OH concentrations at Mace Head during the NAMBLEX campaign. Solid line is the best-fit line with a correlation coefficient of 0.596. The dashed line shows 1 : 1 relationship.

dominated by primary production (*i.e.* formation of $O(^1D)$ atoms and their reaction with water vapour).[24] Moreover, the halogen impact upon HO_x is only expected to be significant under low NO_x conditions, and halogen activity is closely correlated with low tide around the solar maximum, thus the total number of days during a campaign when iodine chemistry could be important is significantly less than the total.

The NAMBLEX OH observations are compared with the calculations of an observationally constrained box model in Fig. 4, which shows the measured OH data and calculations from a model constrained to measured O_3, H_2O, CO, CH_4, NO_x, hydrocarbons, photolysis frequencies and aerosol loading.[25,26] The model reproduces both the diurnal cycle of OH and the day-to-day variability, with a statistically insignificant tendency to slightly overestimate the measured concentrations (mean model to measurement ratio is 1.02 ± 0.03).

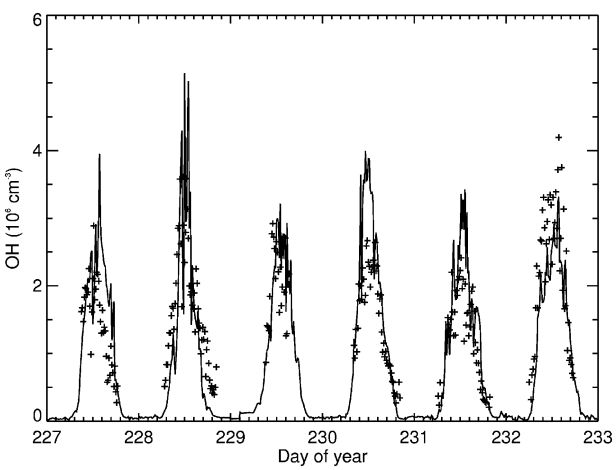

Fig. 4 Comparison of measured OH (points) with the output of an observationally constrained photochemical box model (continuous line) for a 6 d period during the NAMBLEX campaign, August 2002.

For long-lived climate gases such as CH_4, the ability of the model to simulate the annual cycle of OH is more important than its ability to simulate day to day variability. An alternative comparison between model and observations for a field campaign can be made by taking an average of the model OH concentrations over an entire campaign period, and comparing with the measurement average over the same period. As synoptic variability is removed, this approach allows comparison between measurements and global CTM model runs from campaigns for which the actual meteorology and/or emissions are unavailable, for example the EASE and SOAPEX campaigns from 1997 and 1999, respectively. A modification must be made to account for the measurement sampling frequency over the 24 h period; particularly during the earlier campaigns more measurements were performed during the day than at night. We therefore determine the overall measurement sampling distribution in hourly bins for each campaign, and apply the same weighting to the hourly model observations to obtain the values for averaging and comparison with observations.

Fig. 5 shows a 30 d running average of the daily mean OH concentration calculated by GEOS-CHEM for 2002 at Mace Head, Ireland (solid line) and the equivalent mean adjusted to match the sampling frequency of the observations during the NAMBLEX campaign (dotted line). The horizontal dotted line shows the mean of this weighted modelled OH over the duration of the NAMBLEX campaign, and may be compared with the mean NAMBLEX OH observations (solid horizontal line, with shaded uncertainty ranges: the inner, darker uncertainty range indicates the (two standard deviation) uncertainty in the measured concentrations expected for a campaign average, as described in section 2; the outer, lighter uncertainty range is the (two standard deviation) variability in the measured values, and indicates the range of OH measurements contributing to the mean values). The model over-estimates the observed OH by a factor of 25%, in agreement with the direct model to measurement comparisons shown in Figs. 2 and 3.

We can evaluate the model's ability to simulate the annual cycle of OH by considering the OH observed during a previous campaign, EASE-97, which also took place at Mace Head during April and May 1997. The mean OH observed during this campaign and the appropriately averaged model output are also shown in Fig. 5. Again, the model overestimates the observations, in this case by 13%. Although not a critical test of the model's ability to simulate the annual cycle in OH (observations in the winter would be more useful), this does suggests that the model reasonably simulates (at least) the spring to summer transition.

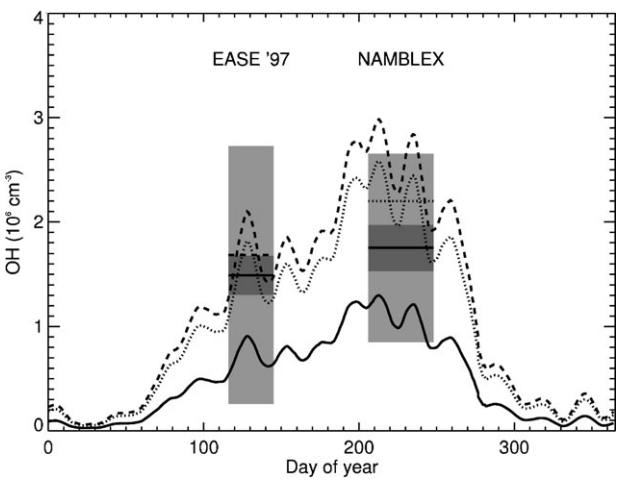

Fig. 5 Plot of modelled 30 d running average OH concentration at the surface at Mace Head over the year (continuous line). Dotted line is calculated from the same model run, but with the hourly data over each 24 h period sampled with the same distribution as the mean measurement distribution over the NAMBLEX campaign, *i.e.* weighted towards daytime measurements. Dashed line is the same model output, sampled using the measurement distribution from the EASE '97 campaign. Continuous horizontal lines are the mean observed OH, lightly shaded areas represent variability in the observed mean (one standard deviation) and the darkly shaded areas the instrumental uncertainty (one standard deviation).

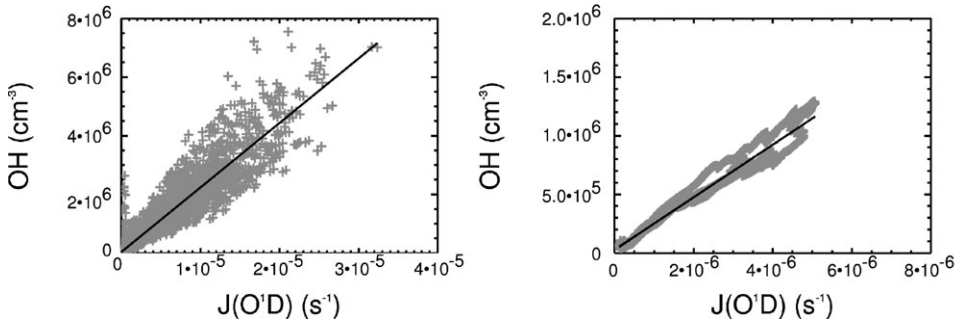

Fig. 6 Simulated $j(O^1D)$ compared with simulated OH from the GEOS-CHEM model at the Mace Head site during 2002. The panel on the left shows hourly data, which has a correlation coefficient of 0.92. The panel on the right shows data with a running 30 d mean to remove diurnal variability and exhibits a correlation coefficient of 0.98.

The large annual variation in OH calculated by the model (Fig. 5) is attributable almost exclusively to changes in the rate of O_3 photolysis, *i.e.* the primary production route for OH. Fig. 6 shows the correlation between the 30 day running mean OH concentration and the 30 day running mean photolysis rate of O_3 to produce $O(^1D)$ atoms, $j(O^1D)$ at Mace Head. The correlation between the hourly simulated $j(O^1D)$ and OH over the year is 0.92 but this mainly reflects the diurnal variability due to day–night transitions and is therefore not particularly interesting. Smoothing the hourly model data with a one month running mean to remove the diurnal and synoptic scales, as for Fig. 5, also leads to an extremely high correlation coefficient of 0.98. Thus, virtually the entire modelled annual variability in OH is attributable to the changing photolysis of O_3 at the Mace Head site. We can apply a similar analysis to the global atmosphere. Fig. 7 shows the correlation coefficient between modelled concentration of OH and modelled $j(O^1D)$. Within the extra-tropics the variation in OH correlates strongly with variations in $j(O^1D)$, with $R > 0.9$. Thus within the model simulation of the extra-tropics virtually all variability in OH concentration can be attributed to variations in O_3 photolysis.

So far only one location in the northern hemisphere has been considered. It would be desirable to compare the model with a wide range of locations across the globe, however the observational data coverage is limited (see section 5) so for simplicity we use a single southern hemisphere location. OH

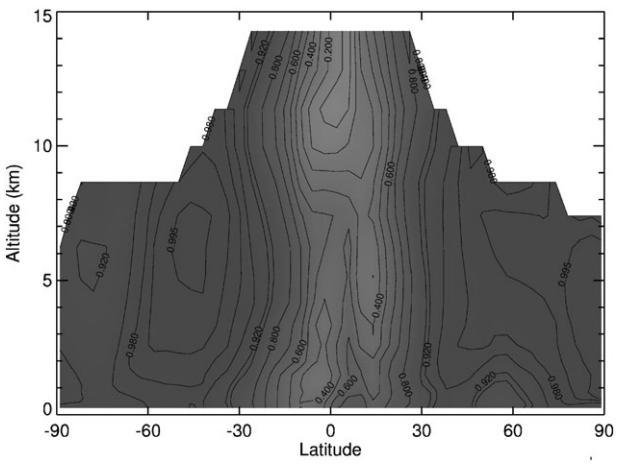

Fig. 7 Zonal mean correlation coefficient between simulated monthly mean $j(O^1D)$ and simulated OH from the GEOS-CHEM simulation for 2002. Within the extra tropics nearly all of the monthly variability in OH is caused by variations in $j(O^1D)$. Within the tropics $j(O^1D)$ is more temporally uniform and other factors control the variability in OH.

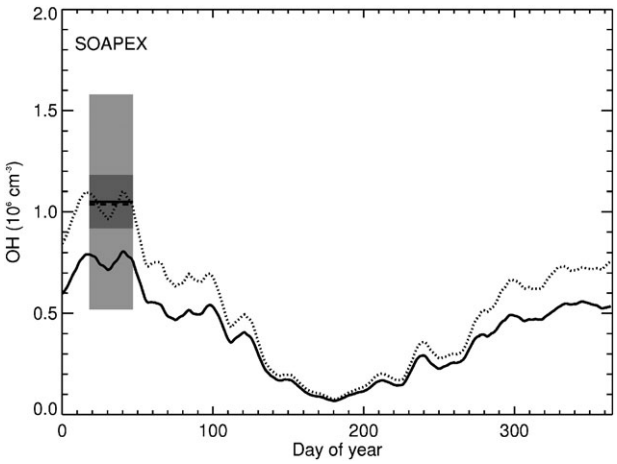

Fig. 8 Plot of modelled 30 d running average of daily mean OH concentration at the surface at Cape Grim, Tasmania employing year 2002 advection and emissions (continuous line). Dotted line is the model output sampled to match the mean 24 hour distribution of the OH observations during the SOAPEX-2 campaign. Continuous horizontal line is the mean of the observed OH, horizontal dashed line is the mean model value over the campaign duration. Shaded errors indicate measurement uncertainty and variability as for Fig. 5.

was measured at Cape Grim, Tasmania during the SOAPEX-2 campaign during January and February 1999. Fig. 8 shows the running mean analysis previously adopted for Mace Head, applied to the SOAPEX-2 campaign data. Again the agreement between the model and observations is good, with the modelled mean OH over the campaign period of 30 d of 1.04×10^6 cm^{-3} comparing favourably with the mean observed concentration of $(1.05 \pm 0.13) \times 10^6$ cm^{-3}.

From the above comparisons, we find that the GEOS-CHEM model agrees with the observed MBL OH concentrations to within at least 25%, which is of the order of the observational uncertainty. The *a priori* modelled global mean OH (as defined earlier) is 1.07×10^6 cm^{-3}. The model appears to satisfactorily calculate the seasonal and geographic variability in OH, at least for the unpolluted mid-latitude locations considered, but the model appears to be systematically high in the northern hemisphere.

The global mean concentration of OH is of central importance to atmospheric chemistry and assessing the consistency of inferred values (from tracer concentrations) and direct measurements (by observation) is important. However, it is difficult to use direct observations, by themselves, to make this assessment; a model is required in order to relate the local observations to a global setting. Despite the geographically restricted nature of the datasets used here, it is possible (with caution) to make an estimate of the global mean OH using a combination of the observations and the model products. We assume that the discrepancies between the modelled and observed OH levels lie with the model, and are systematic in nature, arising from chemical mechanistic shortcomings, inaccuracies in emissions, the calculation of photolysis rates *etc*. Consequently we assume that we can account for the discrepancies, and optimise the modelled global mean OH, by scaling the model OH field to match the (campaign mean) observations. Due to the restricted observational datasets we scale the model OH concentrations using annual mean hemispheric values of $-19 \pm 19\%$ and $+1 \pm 13\%$ for the northern and southern hemisphere, respectively (values are the mean model to measurement ratios from the EASE-97 and NAMBLEX campaigns for the northern hemisphere, and the SOAPEX-2 campaign for the southern hemisphere). This leads to an *a posteriori* (consistent with both the direct *in situ* observations and the OH distribution calculated by the model) value for the global mean OH concentration of $(0.98 \pm 0.16) \times 10^6$ cm^{-3}. The refined uncertainty range reflects the uncertainty in the observed data used to provide the model constraint. The hemispheric *a posteriori* OH is 0.91×10^6 cm^{-3} within the northern hemisphere and 1.03×10^6 cm^{-3} within the southern. These, *a posteriori* hemispheric mean OH concentrations are very close to those calculated by Prinn *et al.*[6] with ratios of 1.04 and 1.01 between our direct assessment of global OH and those of Prinn *et al.*[6] for the northern and southern hemispheres, respectively.

The closeness of the agreement between our *a posteriori* global and hemispheric mean OH and those calculated by Prinn *et al.*[6] is probably fortuitous as it seems unlikely that single surface mid-latitude sites are representative of a whole hemisphere. However, it does indicate that direct observations of OH can be used to help constrain our understanding of the global oxidizing capacity of the atmosphere. The robustness of our analysis could be considerably enhanced by the inclusion of other OH observations. Also, the location or timing of future field campaigns should be targeted to complete gaps in our knowledge. We discuss these needs below.

5. Discussion

From the analysis presented earlier, it appears that our understanding (as manifested by the GEOS-CHEM model) of atmospheric processes controlling OH concentrations (chemistry, photolysis, transport, emissions *etc.*) within mid-latitude marine boundary, is consistent (within the uncertainty) with the observations. However, there is some indication from both the *in situ* and tracer derived techniques that the model systematically overestimates northern hemispheric OH levels. That there is some degree of agreement between the model and observation is largely to be expected. Accurately simulating OH concentrations and distribution is a primary objective of global models. After many years of development, it would be surprising if they failed to produce a relatively realistic simulation of the tropospheric photochemical system, especially as HO_x production and loss is tightly coupled to O_3 production and loss and to NO_x loss with a variety of negative feedbacks maintaining the concentrations of all these species. Such controls may largely explain the success of global atmospheric models of chemical composition. Errors in one aspect of the model may counterbalanced by the negative feedbacks from others. Much of the model success in this work may however be attributed to the simple nature of the photochemistry and the direct dependence of OH concentrations upon $j(O^1D)$ (Figs. 6 and 7). The observational data used (from Mace Head and Cape Grim, remote marine boundary layer locations) are obtained predominantly under conditions in which the main co-reactants for OH are CH_4 and CO, and the main production route for OH is *via* $j(O^1D)$, with little feedback from HO_2 through reaction with NO and O_3 (levels of both of which are low in the remote MBL).

In tuning the modelled global annual mean OH to match the campaign-averaged observed values, we assume that the discrepancy between the two lies with the model, and further that the discrepancy is constant in time and space across each hemisphere. The raw model performance is very good (Figs. 5 and 8), relative to the systematic uncertainty in the observations, and arguably no tuning of the model calculated OH is required. The case for tuning the model OH field could be strengthened by reducing, or better defining, the systematic error in the OH measurements. Also a better assessment of model uncertainty under different photochemical regimes would also provide useful information, however a systematic understanding of the model uncertainty is currently beyond our computational resources.

From the perspective of climate, rather than the actual OH concentration, the rate of removal of key species such as CH_4 is critical. Fig. 9 shows the relative contributions of different regions of the troposphere to the removal of CH_4, as a function of time of year, as calculated by GEOS-CHEM. Unsurprisingly, the tropics dominate the loss of CH_4 with 80% of global CH_4 being removed within this region. The high temperature sensitivity of the reaction between CH_4 and OH ($k = 2.45 \times 10^{-12}e^{(-1775/T)}$ cm^{-3} s^{-1})[27] leads to the rate constant at the tropical surface ($\sim$300 K) being 24 times that at the tropical tropopause ($\sim$195 K). The lowermost part of the tropical troposphere thus plays a disproportionately important role in the removal of CH_4, and to best define the global oxidizing capacity observations should be made in the tropics. Although observations of OH throughout the depth of the tropical troposphere would be most useful, observations made from the surface would still provide critical information about the oxidizing capacity of the atmosphere (as measured by the loss of CH_4).

Fig. 10 shows the dates and locations of previous field campaigns in which OH was measured,[2] horizontal lines represent surface fixed sites, hatched areas denote airborne or ship borne measurements. Fig. 10 also shows the monthly mean column integrated zonal averaged tropospheric OH from GEOS-CHEM. Given the importance of the tropics in determining the oxidizing capacity of the atmosphere it is somewhat unfortunate that the existing observational campaigns have focussed so extensively on northern hemisphere mid-latitude summer/autumn. The tropics are

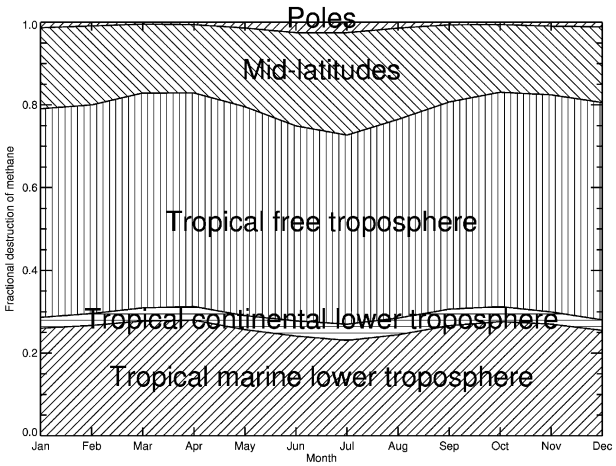

Fig. 9 Contribution of different regions of the troposphere to the total removal rate of CH_4 throughout the year, as calculated by GEOS-CHEM. Tropics defined as 30° S to 30° N, mid-latitudes defined as 30° S to 60° N/S and poles defined as 60° to 90° N/S. The troposphere is defined as the region below 2 km in altitude. The free troposphere is the region from 2 km to the tropopause.

overwhelmingly the most important region for global oxidizing capacity but have in comparison been rather sparingly observed.

Fig. 10 also highlights the sparse temporal nature of the OH measurements, which are typically made during intensive field campaigns. Prinn *et al.*[6] have suggested that global tropospheric OH has

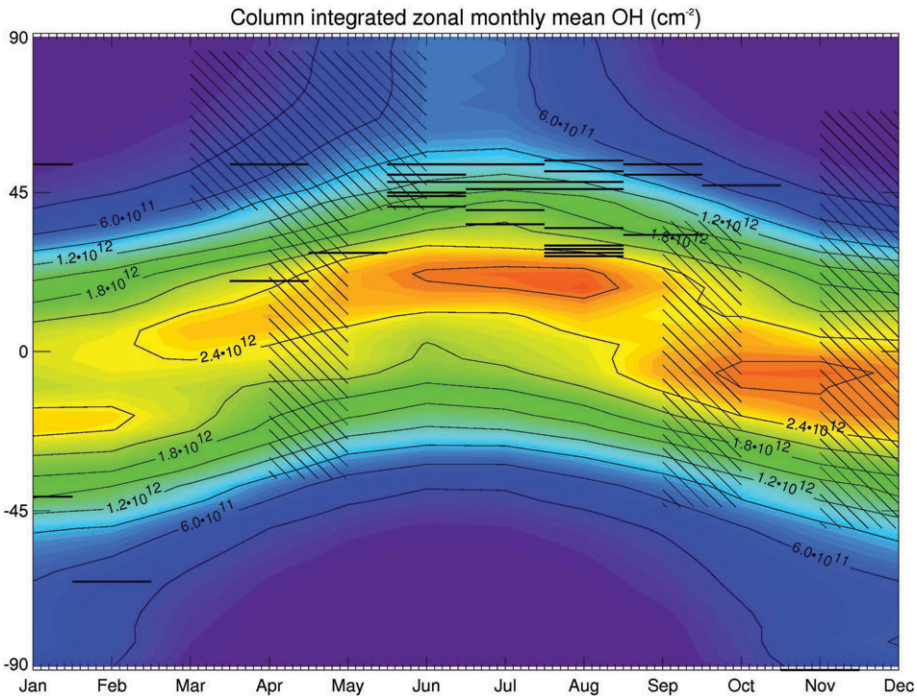

Fig. 10 Seasonal cycle in monthly mean zonal column mass weighted OH from GEOS-CHEM; contour lines represent intervals of 3×10^{11} cm^{-2}. Additional features indicate dates/locations of previous field campaigns in which OH was measured; horizontal lines represent fixed sites, hatched areas denote airborne measurements.

declined over the period 1992–2000, based upon their inversion studies. This is a potentially significant result as it leads to increased lifetimes for many climate gases and hence increases their global warming potentials. However, the sporadic nature of the direct observations of OH do not allow this to be evaluated directly as suitable datasets do not exist.

An enhanced observational network for OH would greatly constrain our understanding of the oxidizing capacity of the atmosphere. This network should be located within the tropics and would ideally be designed to monitor long term trends. Although vertical profiles would offer the largest constraints, the temperature sensitivity of CH_4 oxidation would allow surface observations to provide a significant constraint on our knowledge

6. Conclusions

The ability of the GEOS-CHEM three-dimensional chemistry and transport model to simulate marine boundary layer OH concentrations has been tested by comparison with *in situ* measurement data from three field campaigns. The model is broadly able to reproduce the measurements from campaigns, and shows comparable performance to an observationally constrained box model.

The model has been compared with measurements from the NAMBLEX and EASE-97 campaigns at Mace Head, Ireland, giving model to measurement ratios of 1.25 and 1.13, respectively. Similar comparisons with observations from the SOAPEX-2 campaign at Cape Grim, lead to a ratio of 1.01. We use the mean model to measurement ratios to scale the model hemispheric OH field, and hence derive a tuned value for the global mean OH, with an observationally-derived uncertainty, of $(0.98 \pm 0.16) \times 10^6$ cm^{-3}. This value is in good agreement with recent determinations of global tropospheric OH concentrations and the hemispheric ratio found from top-down tracer inversions.

The model tuning procedure could be further improved through comparison with more field measurement datasets; however, examination of the available data shows a bias towards mid-latitude Northern hemispheric sites, while the global oxidation rate of CH_4 and other hydrocarbons is dominated by the tropics. There is a clear need to obtain further datasets in the tropical regions, to assess our understanding of their photochemical environment, and hence the global oxidative capacity.

Acknowledgements

We thank the NERC for funding the EASE '97, SOAPEX and NAMBLEX experiments and for MJE's Research Fellowship. We thank the research groups associated with these field campaigns for providing the auxiliary information necessary for this study. The GEOS-CHEM model is based in Daniel Jacob's group at Harvard University and is supported by the NASA Atmospheric Chemistry Modeling and Analysis Program.

References

1 H. Levy, *Science*, 1971, **173**, 141.
2 D. E. Heard and M. J. Pilling, *Chem. Rev*., 2003, **103**, 5163.
3 R. G. Prinn, D. M. Cunnold, P. G. Simmonds, F. N. Alyea, R. Boldi, D. Gutzler, D. Hartley, R. Rosen and R. A. Rasmussen, *J. Geophys. Res*., 1992, **97**, 2445.
4 R. G. Prinn, R. F. Weiss, B. R. Miller, J. Huang, F. N. Alyea, D. M. Cunnold, P. J. Fraser, D. E. Hartley and P. G. Simmonds, *Science*, 1995, **269**, 187.
5 M. Krol, P. J. van Leeuwen and J. Lelieveld, *J. Geophys. Res*., 1998, **103**, 10697.
6 R. Prinn, G. J. Huang, R. F. Weiss, D. M. Cunnold, P. J. Fraser, P. G. Simmonds, A. McCulloch, C. Harth, P. Salameh, S. O. Doherty, R. H. J. Wang, L. Porter and B. R. Miller, *Science*, 2001, **292**, 1882.
7 S. A. Montzka, C. M. Spivakovsky, J. H. Butler, J. W. Elkins, L. T. Lock and D. J. Mondeel, *Science*, 2000, **288**, 500.
8 M. C. Krol, J. Lelieveld, D. E. Oram, G. A. Sturrock, S. A. Penkett, C. A. M. Brenninkmeijer, V. Gros, J. Williams and H. A. Scheeren, *Nature*, 2003, **421**, 131.
9 T. Cvitas and D. Kley, *The TOR Network – A Description of TOR Measurement Stations*, Fraunhofer Institute for Environmental Research, Garmisch-Partenkirchen, 1994.
10 T. S. Bates, B. J. Huebert, J. L. Gras, F. B. Griffiths and P. A. Durkee, *J. Geophys. Res*., 1998, **103**, 16297.
11 T. M. Hard, R. J. O'Brien, Y. C. Chan and A. A. Mehrabzadeh, *Environ. Sci. Technol*., 1984, **18**, 768.

12 D. J. Creasey, P. A. Halford-Maw, D. E. Heard, M. J. Pilling and B. J. Whittaker, *J. Chem. Soc., Faraday Trans.*, 1997, **93**, 2907.
13 D. J. Creasey, G. E. Evans, D. E. Heard and J. D. Lee, *J. Geophys. Res.*, 2003, **108**, DOI: 10.1029/2002JD003206.
14 W. J. Bloss, T. J. Gravestock, D. E. Heard, T. Ingham, G. P. Johnson and J. D. Lee, *J. Environ. Monit.*, 2003, **5**, 21.
15 U. Aschmutat, M. Hessling, F. Holland and A. Hofzumahaus, in *Physico-Chemical Behaviour of Atmospheric Pollutants, Report EUR 15609*, ed. G. Angeletti and C. Restelli, Office for Official Publications of the European Communities, Luxembourg, 1994, p. 811.
16 W. J. Bloss, J. D. Lee, C. Bloss, K. Wirtz, M. Martin-Reviejo, M. Siese, D. E. Heard and M. J. Pilling, *Atmos. Chem. Phys.*, 2004, **4**, 571.
17 I. Bey, D. J. Jacob, R. M. Yantosca, J. A. Logan, B. Field, A. M. Fiore, Q. Li, H. Liu, L. J. Mickley and M. Schultz, *J. Geophys. Res.*, 2001, **106**, 23073.
18 A. M. Fiore, D. J. Jacob, I. Bey, R. M. Yantosca, B. D. Field, A. C. Fusco and J. G. Wilkinson, *J. Geophys. Res.*, 2002, **107**, DOI: 10.1029/2001JD000982.
19 R. V. Martin, D. J. Jacob, R. M. Yantosca, M. Chin and P. Ginoux, *J. Geophys. Res.*, 2002, **108**, DOI: 10.1029/2002JD002622.
20 R. J. Park, D. J. Jacob, B. D. Field, R. M. Yantosca and M. Chin, *J. Geophys. Res.*, 2004, **109**, DOI: 10.1029/2003JD004473.
21 C. M. Spivakovsky, J. A. Logan, S. A. Montzka, Y. J. Balkanski, M. Foreman-Fowler, D. B. A. Jones, L. W. Horowitz, A. C. Fusco, C. A. M. Brenninkmeijer, M. J. Prather, S. C. Wofsy and M. B. McElroy, *J. Geophys. Res.*, 2000, **105**, 8931.
22 L. J. Carpenter, W. T. Sturges, S. A. Penkett, P. S. Liss, B. Alicke, K. Hebestreit and U. Platt, *J. Geophys. Res.*, 1999, **104**, 1679.
23 A. Saiz-Lopez and J. M. C. Plane, *Geophys. Res. Lett.*, 2004, **31**, DOI: 10.1029/2003GL019215.
24 W. J. Bloss, J. D. Lee, G. P. Johnson, D. E. Heard, R. Sommariva, J. M. C. Plane, A. Saiz-Lopez, G. McFiggans, H. Coe, M. Flynn, P. Williams, A. Rickard and Z. Fleming, *Geophys. Res. Lett.*, 2004, submitted.
25 R. Sommariva, A. L. Haggerstone, L. J. Carpenter, N. Carslaw, D. J. Creasey, D. E. Heard, J. D. Lee, A. C. Lewis, M. J. Pilling and J. Zádor, *Atmos. Chem. Phys.*, 2004, **4**, 839.
26 R. C. Sommariva, *Understanding Field Measurements through a Master Chemical Mechanism*, PhD Thesis, University of Leeds, 2004.
27 S. P. Sander, R. R. Friedl, D. M. Golden, M. J. Kurylo, R. E. Huie, V. L. Orkin, G. K. Moortgat, A. R. Ravishankara, C. E. Kolb, M. J. Molina and B. J. Finlayson-Pitts, *Chemical Kinetics and Photochemical Data for use in Atmospheric Studies Evaluation #14, NASA-JPL Publication 02–25*, Jet Propulsion Laboratory, Pasadena, CA, 2003.